2-1-1999

Orbitally-Tuned Sr Isotope Chemostratigraphy for the Late Middle to Late Miocene

E. E. Martin
University of Florida

N. J. Shackleton
University of Cambridge

J. C. Zachos
University of California, Santa Cruz

Benjamin P. Flower
University of South Florida, bflower@marine.usf.edu

PALEOCEANOGRAPHY, VOL. 14, NO. 1, PAGES 74-83, FEBRUARY 1999

Orbitally-tuned Sr isotope chemostratigraphy for the late middle to late Miocene

E.E. Martin,[1] N.J. Shackleton,[2] J.C. Zachos,[3] and B.P. Flower[4]

Abstract. We present a Sr chemostratigraphic reference section for the late middle to late Miocene (14-5 Ma) from Ocean Drilling Program site 926 on the Ceara Rise. This site combines a precise, orbitally tuned timescale with a high sedimentation rate (15 m/m.y.), continuous deposition, and excellent biostratigraphic control. The Sr isotope curve is based on measurements of cleaned, planktonic foraminifera at 100-200 kyr sample intervals and it illustrates periods of rapid change in $^{87}Sr/^{86}Sr$ alternating with periods of little change. Chemostratigraphically-defined ages for these intervals can be determined within +/-0.8 m.y. and +/-1.6 m.y. respectively. There is excellent correlation with the published curve for site 588 [*Hodell and Woodruff*, 1994]; however the curve for site 747 [*Oslick et al.*, 1994] exhibits less structure, which may be due to small errors in age estimates related to slow sedimentation rates, high-latitude fauna and an interval of complicated magnetics. Late Miocene data compare favorably with data from site 758 [*Farrell et al.*, 1995].

1. Introduction

Sr isotope chemostratigraphy represents a reliable and straightforward technique for correlating marine sediments globally [*Burke et al.*, 1982; *DePaolo and Ingram*, 1985; *Hess et al.*, 1986; *Palmer and Elderfield*, 1985; *Hodell et al.*, 1989; *Hodell and Woodruff*, 1994; *Mead and Hodell*; 1995; *Oslick et al.*; *Miller et al.*, 1991; *Farrell et al.*, 1995]. The accuracy of this technique is determined by the slope of the curve, the precision with which the exact values and shape of the curve are known, and the external precision of the Sr isotope analyses to be compared to the established curve. For intervals of the curve with rapidly changing $^{87}Sr/^{86}Sr$ values the resolution is ~+/-0.5 m.y., which rivals biostratigraphic resolution [*Miller and Kent* , 1987]; however, for intervals of the curve representing little change in $^{87}Sr/^{86}Sr$ with time, other stratigraphic techniques tend to yield more precise estimates. The advantages to Sr isotope chemostratigraphy over biostratigraphy and magnetostratigraphy are that it can be applied to (1) any sample that contains a small amount of contemporaneous marine carbonate, (2) regions where endemic fauna may be difficult to correlate, and (3) sections that have poor magnetic records.

Variations in seawater Sr isotopes reflect changes in the flux or isotopic ratio of two primary end-members: radiogenic Sr eroded from the continents and less radiogenic Sr supplied through hydrothermal alteration of ocean crust. A third source, dissolution of marine carbonates, predominantly buffers the seawater Sr system. Variations in Sr supplied from continental and oceanic crusts are caused by changes in (1) the rate of material weathered from the continents, (2) the type of material exposed to weathering on the continents, and (3) the extent of hydrothermal alteration of ocean crust [*Elderfield*, 1986; *Hodell*, 1994]. Therefore inflection points in the seawater curve provide a record of tectonism and climate change. They also provide useful tie points for chemostratigraphic correlations because they provide a mechanism for correlating curves by their shape rather than their absolute isotopic values.

The ideal Sr isotope chemostratigraphic reference section would consist of a site with rapid sedimentation for high resolution and a well-defined magnetostratigraphy for correlation to absolute ages on the geomagnetic polarity timescale (GPTS). Unfortunately, these two properties tend to be mutually exclusive in marine sediments: sites with rapid sedimentation rates, such as equatorial regions, generally have weak remanent magnetization, and sites with well-defined paleomagnetic records exhibit low sedimentation rates. An alternative method for precise dating is to astronomically "tune" sediments that exhibit cyclic sedimentation patterns related to orbital cycles [*Imbrie et al.*, 1984; *Hilgen et al.*, 1995; *Shackleton et al.*, 1995].

During Ocean Drilling Program (ODP) Leg 154 it was discovered that upper middle Miocene and upper Miocene sediments from site 926 demonstrated strong cyclicity based on color, magnetic susceptibility, and natural gamma ray emission [*Curry et al.*, 1995]. These properties were used to develop a timescale for this portion of site 926 by correlating the observed cyclicity to astronomical variations in Northern Hemisphere summer insolation [*Shackleton and Crowhurst*, 1997]. Sr isotope analyses were then plotted against orbitally tuned ages to produce a Sr chemostratigraphic reference section. This reference section therefore combines the optimum conditions of rapid sedimentation rates (14-18 m $m.y.^{-1}$) and well-defined absolute age control linked to the GPTS. In addition, this site exhibits remarkably continuous deposition for the late middle to late Miocene and excellent biostratigraphic control that can be tied into numerous low-latitude sites. Finally, the Sr data can be linked to well-

[1] Department of Geology, University of Florida, Gainesville.
[2] Earth Sciences Department, University of Cambridge, Cambridge, England, United Kingdom.
[3] Earth Sciences Department, University of California at Santa Cruz.
[4] Department of Marine Sciences, University of South Florida, St. Petersburg.

Paper number 1998PA900008.
0883-8305/99/1998PA900008$12.00.

documented oxygen and carbon isotope stratigraphies [*Flower et al.*, 1997; *Shackleton and Hall*, 1997], which ultimately will be important for understanding the mechanisms controlling the Sr isotopic variations.

The middle Miocene portion of the reference section also overlaps with Sr curves produced from site 588 by *Hodell and Woodruff* [1994], (hereinafter referred to as HW) and site 747 by *Oslick et al.* [1994], (hereinafter referred to as OMWF). Although the data from HW and OMWF generally overlap within error, there is an offset of variable magnitude between the two that can result in differences in age estimates of up to 1.8 m.y. One of our objectives is to elucidate this discrepancy between data sets.

2. Methods

ODP site 926 (3°43'N, 42°54'W) was drilled at intermediate bathymetric depths (3.6 km) during a transect taken on the Ceara Rise in the western equatorial Atlantic during Leg 154 [*Curry et al.*, 1995] (Figure 1). The site sits above the modern lysocline, but increased evidence of dissolution in the Miocene section suggests a shallower lysocline at that time. The sediment is primarily composed of a moderately indurated, clayey nannofossil chalk. This lithification, combined with the pore water geochemistry [*Hampt and Delaney*, 1997], indicates slight bulk carbonate recrystallization. However, scanning electron micrographs reveal that the planktonic foraminifera tests are free of calcite overgrowths (Figure 2). In addition, $\delta^{18}O$ values within expected ranges and Sr concentration data argue against diagenetic alteration of the foraminfers [*Flower et al.*, 1997].

Three holes (926A, 926B, and 926C) were cored at this site, and a good composite depth scale was created to 300 m composite depth [*Curry et al.*, 1995]. Like most equatorial sediments, site 926 does not preserve a clean paleomagnetic signal. Strong, drilling-induced overprinting eliminated any potential for magnetostratigraphy. However, there are abundant calcareous nannofossils and foraminifera that provided excellent low-latitude biostratigraphies. In addition, the sediments from site 926 are characterized by an obvious visual cyclicity, as well as cyclicities in magnetic susceptibility and measured reflectance, all of which are driven by variations in the ratio of terrigenous material to biogenic carbonate [*Curry et al.*, 1995]. *Shackleton and Crowhurst* [1997] demonstrated that these cycles are related to variations in Northern Hemisphere summer insolation on precession timescales. On the basis of this observation they produced an orbitally tuned timescale for site 926 sediments from 14 to 5 Ma. Errors are estimated to be at the level of an individual precession cycle.

Samples were analyzed for intervals representing ~200 kyr for 14-9 Ma and every 100 kyr for 9-5 Ma. For the Sr isotope analyses, 300-500 μg of planktonic foraminifera were picked from the >150-μm fraction. Each chamber was broken open and the pieces sonicated in quartz-distilled water in order to remove any internal clay. The cleaned fragments were then dissolved in 1.8N HCl. The solution was dried, dissolved in 50 μL 3.5 HNO_3, and loaded onto Sr selective crown ether resin. The Sr was separated using a technique modified from *Pin and Bassin* [1992]. Our Sr blank for this technique is 100 pg. The Sr was then loaded with tantalum oxide onto tungsten filaments and analyzed for $^{87}Sr/^{86}Sr$ on a VG Micromass 354 triple collector thermal ionization mass spectrometer in dynamic mode. Two hundred ratios were collected at 1.5 V. Mass fractionation was corrected to $^{87}Sr/^{86}Sr = 0.1194$. The measured $^{87}Sr/^{86}Sr$ value and external precision for National Institute of Standards and Technology (NIST)-987 standards run in the lab at the University of Florida (UF) are 0.710235 +/- 0.000023. This external precision is equivalent to the 2σ uncertainty based on replicate analyses of NIST-987 over a period of several years, and it represents the minimum uncertainty assigned to any individual sample, although within-run uncertainties were considerably lower (0.000009 - 0.000016). Nineteen sets of replicate samples were also analyzed during this study (Table A1)[1]. The variation between replicates ranged from 0.000001 to 0.000042, and averaged 0.000019, which is consistent with the stated external error based on NIST-987 analyses.

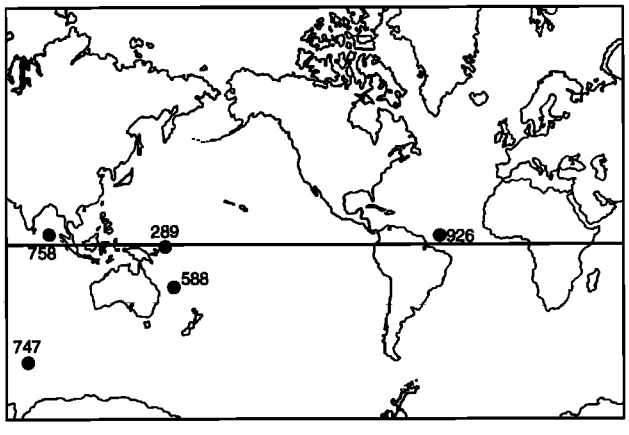

Figure 1. Location map for sites discussed in the text.

3. Results

Sr isotopes are plotted versus composite depth (Table A1) in Figure 3 for the entire Miocene section. The portion of the section that has been orbitally tuned spans from 300 to 154 m. It is clear from these data that there is an unconformity below the tuned section at ~330 m [*Flower et al.*, 1997] that was not detected by shipboard examination. From ~490 meters composite depth (mcd) to the hiatus at 330 mcd the Sr isotopes increase quite rapidly. Above the hiatus the curve alternates between sections with very little change in $^{87}Sr/^{86}Sr$ from 329.5 to 263.91m and 221.3 to 183.2 m, and sections with more rapid change from 261.5 to 222.6 m and 181.3 m to the top of the section at 153.9 m.

[1] Table A1 is available on diskette or via Anonymous FTP from kosmos.agu.org, directory APEND (Username=anonymous, Password=guest). Diskette may be ordered by mail from AGU, 2000 Florida Avenue, NW, Washington, DC 20009 or by phone at 800-966-2481; $15.00. Payment must accompany order.

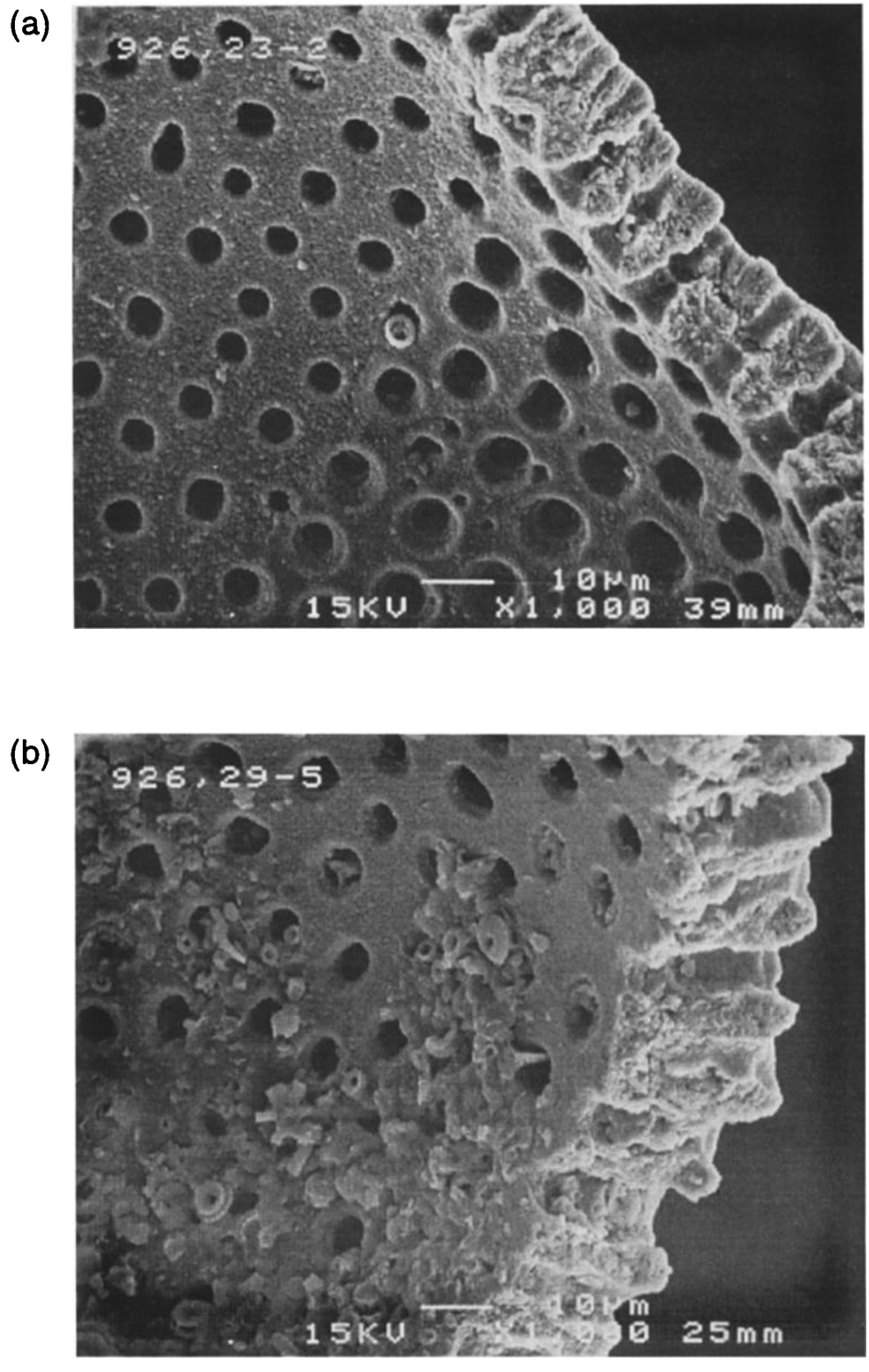

Figure 2. Scanning electron micrographs of the interiors and cross sections of foraminifera tests from site 926. (a) A specimen from 926A, 23-2, 98-100 cm (230.05 meters composite depth (mcd)), magnified 1100 times. This interval is within the nannofossil ooze lithology of unit II and illustrates the very clean nature of the samples. (b) A specimen from one of the deepest astronomically tuned samples, 926B, 29x-5, 44-46cm (295.26 mcd), magnified 1000 times. This sample is from the nannofossil chalk of unit III. Some adhering carbonate sediment is visible, mostly composed of coccoliths, but there is no evidence of crystal overgrowths.

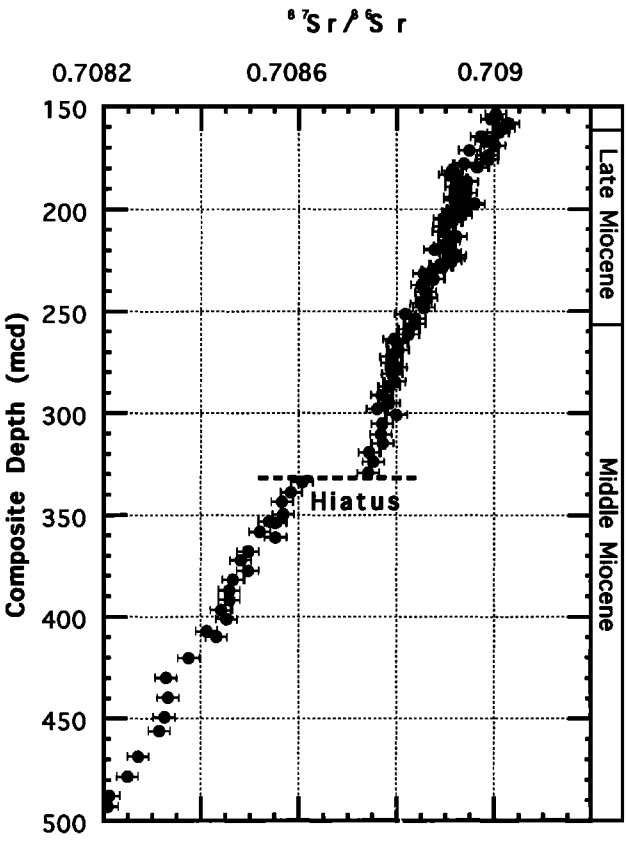

Figure 3. The Sr isotope record of the entire Miocene section for Ocean Drilling Program (ODP) site 926 versus composite depth. A hiatus is apparent at 330 m [*Flower et al.*, 1997]. The section from 154 to 300 m has been orbitally tuned.

4. Discussion

4.1. Comparison to Published Data Sets

We have used two different methods to compare site 926 data to published seawater Sr isotope curves. The first is to construct an age model for site 926 using ages derived from a comparison of Sr isotope values to published seawater curves. The second is to make a direct comparison of the seawater Sr isotope curves for the portion of site 926 that is astronomically tuned. As mentioned, both HW and OMFW published detailed Sr seawater curves for the early to late Miocene. These two sites are characterized by extremely different sedimentation rates. The sedimentation rate for site 747 ranges from ~7 m m.y.$^{-1}$ in the middle Miocene to 6 m m.y.$^{-1}$ in the late Miocene (OMWF). Rates are 2-3 times more rapid at site 588, where the middle Miocene was deposited at roughly 14 m/m.y. and the late Miocene was deposited at 22 m m.y.$^{-1}$ (HW). Rates for site 926 are very similar to those of site 588 (14 m m.y.$^{-1}$ in the middle Miocene and 18 m m.y.$^{-1}$ in the upper Miocene). The stratigraphies for both sites 588 and 747 are based on paleomagnetics, with the addition of oxygen and/or carbon isotope events (HW and OMWF). At site 588, paleointensities are very low above ~8.5 Ma; however, the pattern of reversals determined by natural remnant magnetization defines a clear magnetostratigraphy [*Barton and Bloemendal*, 1986]. It should be noted that ages for the portion of the HW curve older than 16 Ma were based on data from site 289. This site contains a poor magnetostratigraphic record; therefore the ages were determined from biostratigraphy as well as the timing of carbon isotope events. We made no correlations to these data because the tuned chronology is currently only available for the sediment younger than 16 Ma.

HW fit the data for site 588 to a ninth-order polynomial. In contrast, OMWF divided their data from site 747 into two linear regressions (Figure 4). The two data sets generally agree within error, meaning the ratios for any given age are the same +/-0.000020, the stated external error for both data sets. In both studies the data span from 23 to 9 Ma. For almost half of this interval (20.8-18 Ma and 13-10 Ma) the offset exceeds the error, ranging from 0.000040 to 0.000060 after normalization to standard values. In addition, the OMFW ratios are consistently higher (Figure 4). The shape and trend produced by the two curves results in age differences of 0.8 m.y. in the early Miocene and 1.8 m.y. in the middle Miocene, such that samples with the same isotopic ratio are consistently older based on the linear regressions established by OMWF. In order to determine whether the statistical treatment of the data influenced the correlation we also fit a ninth-order polynomial to the data from site 747, but this did not alter the correlation.

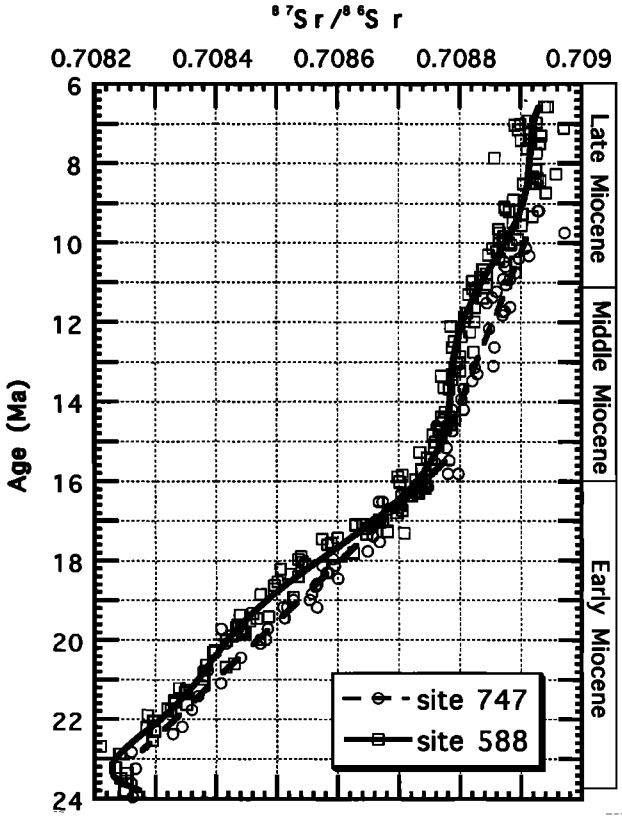

Figure 4. Comparison of Miocene seawater $^{87}Sr/^{86}Sr$ data for site 588 [*Hodell and Woodruff*, 1994] and site 747 [*Oslick et al.*, 1994]. The solid line represents a ninth-order polynomial fit to the 588 data; the dashed lines represent two linear regression fits to the 747 data. The timescale for both data sets is *Cande and Kent* [1992]. All data are normalized to our National Institute of Standards and Technology (NIST)-987 value of 0.710235.

The offset between the two curves was noted at the time of publication, samples were exchanged and an interlaboratory comparison was made (HW and OMWF). A total of 6 samples from site 747 were analyzed at UF, and 10 samples from site 588 were analyzed at Rutgers. After all the analyses are normalized to reported NIST-987 and seawater standard values the samples from Rutgers still average 0.000020 higher; suggesting that a portion of the offset observed between the two curves may be attributed to an interlaboratory bias that was not accounted for by normalization to standards. However, an additional 0.000020-0.000040 difference must be attributable to some other cause, such as diagenesis or errors in age assignment. A cause other than interlaboratory bias is supported by the fact that the offset between the two curves is variable.

To determine which data set is most compatible with the site 926 data, we derived an age for each Sr isotopic measurement from site 926 using the polynomial fit for site 926 (HW) and the linear regressions for site 747 (OMFW) (Table A1). It was then possible to plot age versus depth models for site 926 on the basis of both sets of derived ages (Figure 5). These two models are compared to biostratigraphic data for site 926. These data include all nannofossil and foraminifera datums reported on shipboard [*Curry et al.*, 1995], as well as additional and revised datums reported by *Pearson and Chaisson* [1997]. The datums viewed as most reliable, and therefore utilized on shipboard to construct an age-depth model, have been highlighted with asterisks. Figure 5 illustrates that ages derived chemostratigraphically from site 588 (HW) more closely approximate the biostratigraphic data for site 926. One point of caution is that the HW and OMFW curves utilize the *Cande and Kent* [1992] timescale, while the timescale applied to the biostratigraphic data from site 926 is from *Shackleton et al.* [1995]. However, the maximum age difference for magnetic anomalies between these two timescales over the time interval of interest is only 0.073 m.y. [*Shackleton et al.*, 1995]. The potential error introduced by comparing data using these two timescales therefore is less than the error generated by the uncertainty in the $^{87}Sr/^{86}Sr$ measurements. In addition, a shift of 0.073 m.y. in any of the data sets would not alter this result.

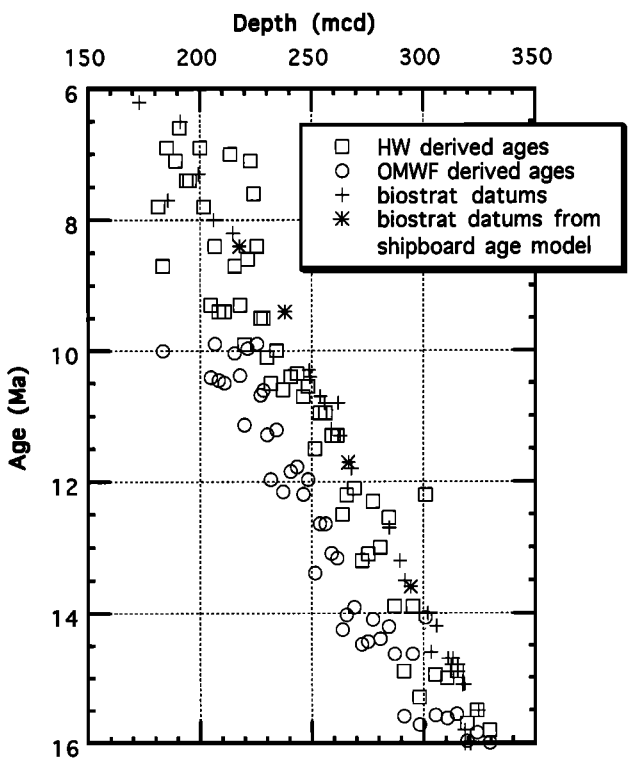

Figure 5. Ages estimated from our $^{87}Sr/^{86}Sr$ data using the calibrations from *Hodell and Woodruff* [1994] and *Oslick et al.* [1994]. Ages based on the *Hodell and Woodruff* [1994] calibration closely track those estimated from biostratigraphy, while those estimated using the *Oslick et al.* [1994] calibration are consistently too old. The pluses represent all of the shipboard biostratigraphic datums [*Curry et al.*, 1995], while the asterisks represent those datums regarded as most reliable and therefore used shipboard to create an age-depth model.

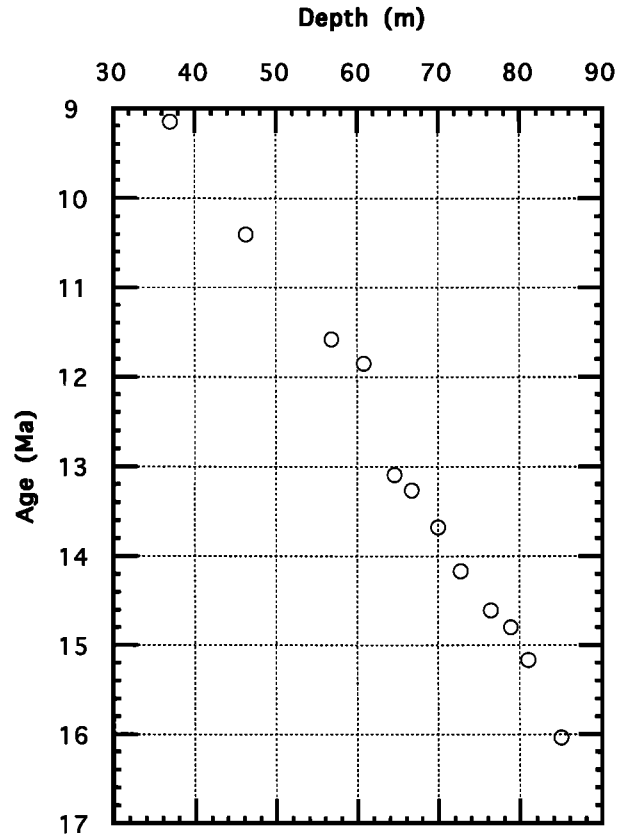

Figure 6. Age model for site 747 based on data in Table A1 from *Oslick et al.* [1994]. The discontinuity at ~12 Ma is in the interval of the greatest discrepancy between ages predicted from sites 588 [*Hodell and Woodruff*,1994] and 747 [*Oslick et al.*, 1994].

In part, the correlation between sites 588 and 926 may be due to the fact that the samples were analyzed on the same mass spectrometer at UF; however, extremely different sample sizes were prepared (1.5 mg for 588 and $\leq$ 500 mg for 926), different separation procedures were utilized (HCl elution with Dowex resin for 588 and HNO_3 and water elution with Sr Spec resin for 926), different loading techniques were applied (tantalum filament for 588 and tantalum oxide on a tungsten filament for 926), and different running conditions were established (2 V for 588 and 1.5 V for 926). Even with these modifications to the preparation technique and running conditions, there has

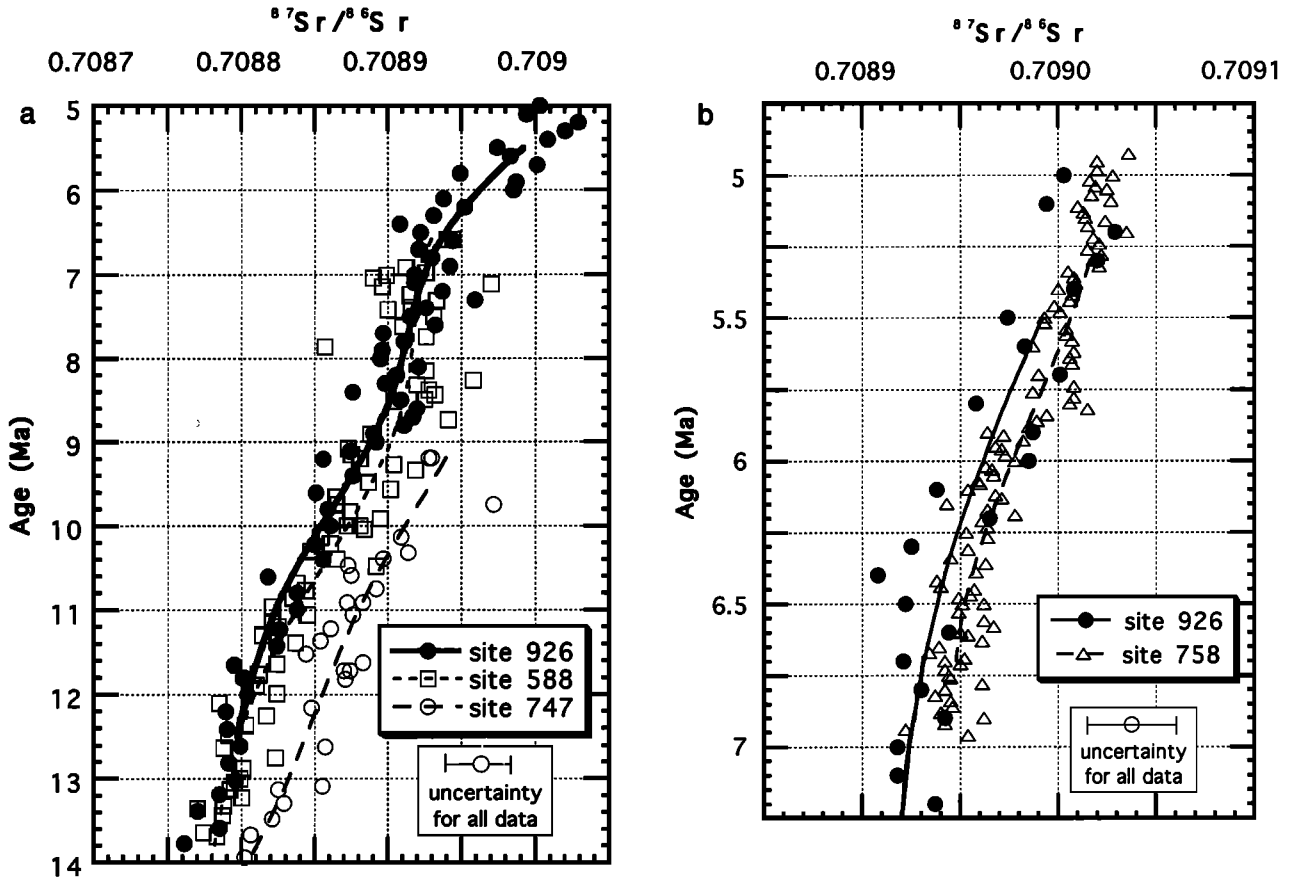

Figure 7. Comparison of published $^{87}Sr/^{86}Sr$ versus age data to the orbitally tuned $^{87}Sr/^{86}Sr$ curve for site 926. (a) The comparison between sites 926, 588 [*Hodell and Woodruff*,1994], and 747 [*Oslick et al.*, 1994] illustrates a good correlation between the shape and values of the curves from sites 588 and 926. In contrast, the curve from site 747 demonstrates almost no structure, and $^{87}Sr/^{86}Sr$ values are ~0.000050 higher. (b) For the younger section, data from sites 926 and 758 [*Farrell et al.*, 1995] overlap within the uncertainty. Polynomial fits to the two data sets have remarkably similar forms; however, site 758 $^{87}Sr/^{86}Sr$ values are ~0.000015 higher, suggesting there may be an interlaboratory bias that has not been accounted for.

been no shift in the measured value of NIST-987 at UF. Thus the comparison between sites 588 and 926 has the advantage of not requiring any interlaboratory correction. However, even after corrections for known and previously unidentified interlaboratory bias, much of the data from site 747 are still consistently higher than the data from sites 588 and 926. This suggests that there is a source of error in site 747 that is distinct from interlaboratory bias.

There is little reason to suspect significant diagenetic alteration at site 747. The foraminifera were recovered from a clean nannofossil ooze with no evidence of secondary overgrowths. Also, because of the slow sedimentation rate, the burial depths are quite shallow (41-130 m). However, the slow sedimentation rate also means that small errors in age determination will be magnified. In addition, many of the low-latitude biostratigraphic marker species are not present at this high-latitude site; therefore the biostratigraphic control is less robust. In Figure 6 a discontinuity in the age model for site 747A (OMFW, Table 1) reveals potential problems in the interval for which there is the biggest discrepancy between the 588/926 and 747 data (~11.5-13 Ma). The magneto-stratigraphy near the middle/upper Miocene boundary at site 747 is described as "uncertain" [*Wright and Miller*, 1992; OMFW, pg. 431], and chron C5AA in the middle Miocene has not even been identified in site 747. Thus much of the offset may be due to miscorrelation in this section; however, it is difficult to reinterpret the magnetostratigraphy in such a way that the isotope patterns match up throughout this interval.

4.2. Orbitally Tuned Timescale

A simpler comparison between the data sets can be made for the section of site 926 that has been orbitally tuned. In this case the $^{87}Sr/^{86}Sr$ versus age curves from HW and OMFW are compared directly to the orbitally tuned Sr chemostratigraphic curve for site 926 (Figure 7a). Again, there is substantial overlap between sites 588 (HW) and 926. In addition, the shapes of the curves are quite similar. In contrast, the $^{87}Sr/^{86}Sr$ values from site 747 (OMFW) are consistently higher for a given age, and the curve for this portion of the data has almost no structure.

Data from site 758 by *Farrell et al.* [1995] cover the younger portion of the section analyzed at site 926. *Farrell et al.* [1995] present a high-resolution $^{87}Sr/^{86}Sr$ curve with a sample

interval of ~0.015 m.y. A plot of $^{87}Sr/^{86}Sr$ versus age from 7.5 to 5 Ma for sites 758 and 926 (Figure 7b) illustrates that the data points from the two data sets overlap within error. In addition, polynomial curves fit to the data demonstrate a remarkable similarity in form; however, there is a slight offset of ~0.000015 in the $^{87}Sr/^{86}Sr$ ratio between the two curves. This small difference in the isotopic ratio translates to an age difference of ~0.2 m.y. This offset is very consistent, suggesting it may again represent an uncorrected interlaboratory bias. As in the comparison to OMFW, the data generated at UF yield consistently lower isotopic ratios for a given age. Also, there is a slight difference in the timescales applied to the two data sets. The curve for site 758 used the timescale by *Shackleton et al.* [1995], while the site 926 data are based on the orbitally tuned timescale; however, the differences between the two timescales is far less than the observed offset.

The data from sites 758 [*Farrell et al.*, 1995] and 926 document a rapid increase in $^{87}Sr/^{86}Sr$ of 0.000050 m.y.$^{-1}$ from 6.5 to 4.9 Ma (Figure 7b); however, in both data sets this rate of increase is approximately half that observed by *McKenzie et al.* [1988] and *Hodell et al.* [1991] for the interval from 5.5 to 4.5 Ma (timescale of *Berggren et al.* [1985], equivalent to 5.95-4.95 on our timescale). As *Farrell et al.* [1995] suggested, this discrepancy appears to be created by inclusion of anomalously low $^{87}Sr/^{86}Sr$ values for site 502 in the older portion of the interval [*McKenzie et al.*, 1988; *Hodell et al.*, 1991], which may be attributed to stratigraphic uncertainties at that site.

In the site 758 data there is a step-like increase from 5.9 to 5.8 Ma. *Farrell et al* [1995] pointed out that additional data would be required to determine whether or not this represents a global change in seawater $^{87}Sr/^{86}Sr$. Data from site 926 lack the very high temporal resolution of the site 758 data; however, the corresponding interval is recorded as a decrease in site 926. We emphasize that this is based on an analysis of only two data points, yet the overall trend of the site 926 data from 6.5 to 5.0 Ma supports the interpretation of a relatively linear increase throughout this interval. In interpreting these high-resolution chemostratigraphic records it is important to remember that the details of the variations in the data on these fine timescales are frequently a function of the uncertainty in the data, rather than actual seawater variations. The study by *Henderson et al.* [1994] illustrates how much care must be taken when interpreting small-scale features.

4.3. Sr Chemostratigraphic Reference Section

The Sr isotope curve from ODP site 926 (Figure 8) is proposed as a chemostratigraphic reference section for the late middle to late Miocene. Unlike other sites evaluated for Sr isotopes, this site incorporates rapid sedimentation for improved age resolution of the curve, an excellent orbitally tuned timescale for improved accuracy, an excellent biostratigraphy for testing the orbital timescale, and continuous deposition. Close correlation to previously published data sets validates the global significance of the reference section.

In the past the Miocene portion of the seawater curve has been approximated by a series of linear segments [*Hodell et al.*, 1991; OMWF] or by higher-order polynomial fits [*Farrell et al*, 1995; HW]. For this data set the difference in age determinations produced by these two techniques is minor; the maximum difference is 0.3 Ma, and it occurs at the end points of the linear regression segments. For a vast majority of the section the difference is ≤0.1 m.y. Because the form of the seawater curve is not necessarily linear, we have chosen to fit the data to a seventh-order polynomial (Figure 8). Nonparametric techniques [*Howarth and McArthur*, 1997] produce a similar curve [*Ludwig et al.*, 1988; *Shackleton and Imbrie*, 1990]; however, we have chosen a polynomial fit for the sake of simplicity and for comparison to previous works. The polynomial curve does not extend to the upper and lower extremes of the data in order to minimize end effects. The curve highlights the lower-frequency variations in seawater $^{87}Sr/^{86}Sr$ with time but neglects whatever information is stored in the higher-order variations. Much of this higher-order signal is a function of analytical uncertainty; however, the curve smoothes the natural as well as the analytical variability; in particular, it may minimize the change in slope at inflection points.

The age of an unknown can be estimated most easily by graphical correlation to the reference section. An iterative calculation based on the seventh-order polynomial equation displayed on Figure 8 is also possible but far more complicated. The error associated with any age estimated from

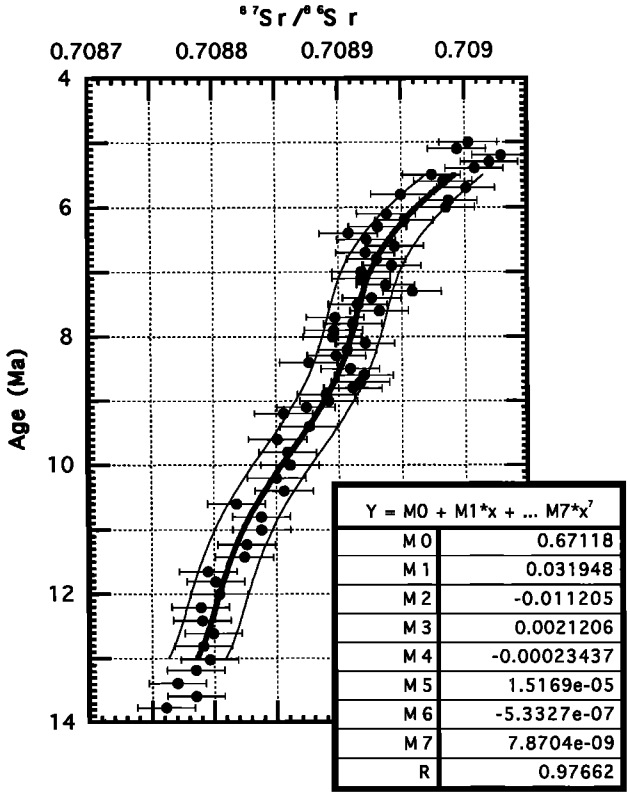

Figure 8. The proposed Sr chemostratigraphic reference section for the late middle and late Miocene from ODP site 926 with ages based on the astronomic timescale by Shackleton. The seventh-order polynomial equation for the curve is given. A conservative error envelope of 0.000023 represents the error associated with the curve fit. An additional analytical error associated with $^{87}Sr/^{86}Sr$ values of unknowns will depend on the accuracy with which those values are known.

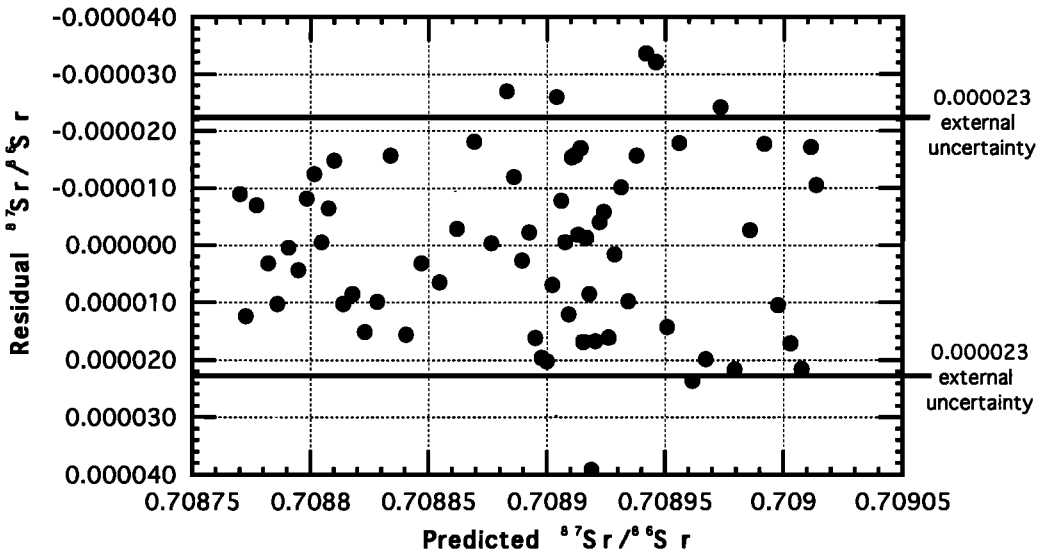

Figure 9. Residual $^{87}Sr/^{86}Sr$ values for the site 926 chemostratigraphic reference section. The residual is equal to the difference between the $^{87}Sr/^{86}Sr$ ratio measured from site 926 and the ratio predicted from the polynomial curve.

the curve is a function of (1) the slope of the curve, (2) the accuracy of the curve fit, which is also influenced by the uncertainty in the $^{87}Sr/^{86}Sr$ measurements and the age model, and (3) the external precision of the $^{87}Sr/^{86}Sr$ value for the sample of unknown age. The accuracy of the curve fit to the polynomial can be viewed visually as a plot of residuals, the difference between $^{87}Sr/^{86}Sr$ values predicted by the polynomial equation and those measured from site 926 samples (Figure 9). Figure 9 illustrates that 59 of the 66 data points (89%) fall within the analytical uncertainty of 0.000023. Also, there is no systematic pattern to the errors, suggesting the error is not autocorrelated. Mathematically, the standard deviation of the residuals is 0.000015, implying that the analytical error associated with each value used to define the curve is greater than the error in the fit of the data to the curve. Therefore we have used an error envelope equivalent to external precision (0.000023) as a conservative estimate of the accuracy of the curve.

The external precision attributed to an unknown can be minimized by running duplicate or triplicate samples. Thus this aspect of the error equals 0.000023 for a single analysis, 0.000016 for duplicate analyses, or 0.000013 for triplicate analyses. Combining the error associated with the curve fit with the error associated with duplicate analyses, the total error in age estimates based on the reference section curve range from +/-0.8 m.y. for intervals of rapidly changing $^{87}Sr/^{86}Sr$ to +/-1.6 m.y. for intervals with little or no change in $^{87}Sr/^{86}Sr$.

Of the residuals that fall outside the range of analytical uncertainty, several are associated with inflection points in the curve (0.708905, 0.708943, and 0.708947), and one (0.708920) represents duplicate analyses that only differed by 0.000010 (sample B19H-6, 14-16 cm). Therefore it is possible that some of the apparent error may be actually due to structure in the curve. Additional analyses from another core are required to confirm this possibility. The inflection points occur at ~11, 8.5, and 6.5 Ma. Future work will compare $^{87}Sr/^{86}Sr$ with other climate proxies to try to understand changes in ocean chemistry associated with variations in weathering fluxes from the continents and hydrothermal circulation.

For some applications the maximum difference in age estimates of 0.3 m.y. between the polynomial and linear fits to the data is insignificant. In these cases, linear regression equations fit to the reference section offer a simpler method for determining age based on $^{87}Sr/^{86}Sr$. For this reason we list the relevant equations below. The linear segments for these regressions were chosen to match most closely the polynomial fit; therefore there are four linear segments that are divided by the inflection points from the seventh-order polynomial fit. The data do not strictly dictate the number of segments or the ages of the divisions between segments. Other linear regressions can also be fit to these data; however, for all other linear equations the difference in ages estimated by the linear versus polynomial fits increases.

The regression for 11-14 Ma has a correlation coefficient (r) of 0.765. The equation is

$$\text{Age (Ma)} = 34{,}742.03 - (^{87}Sr/^{86}Sr)48{,}997.99 \quad (1)$$

The r value for 8.5-11 Ma is 0.848, and the equation is

$$\text{Age (Ma)} = 20{,}959.92 - (^{87}Sr/^{86}Sr)29{,}554.32 \quad (2)$$

The r value for 6.5-8 Ma is 0.575, and the equation is

$$\text{Age (Ma)} = 33{,}904.08 - (^{87}Sr/^{86}Sr)47{,}814.86 \quad (3)$$

Finally, the r value for 6.5-5 Ma is 0.797, and the equation is

$$\text{Age (Ma)} = 10{,}727.57 - (^{87}Sr/^{86}Sr)15{,}123.10 \quad (4)$$

5. Conclusions

The ideal site for development of a Sr chemostratigraphic reference section would combine a rapid sedimentation rate for improved resolution with well-dated sediments that can be linked to the GPTS. Unfortunately, high sedimentation sites are notorious for having poor magnetic records. In order to resolve this disparity, we developed a Sr chemostratigraphic reference section for the late middle to late Miocene (14 to 5 Ma) at site 926, a low-latitude site on the Ceara Rise, using a very precise, orbitally tuned timescale.

Comparison of the site 926 $^{87}Sr/^{86}Sr$ data with previous data for this time interval indicates that there is a better correlation to the data from site 588 [*Hodell and Woodruff*, 1994] than from site 747 [*Oslick et al.*, 1994]. The shapes of the site 926 and 588 curves are similar, and the absolute values for any point on the curve are within the analytical uncertainty. In contrast, the magnitude of the difference between sites 926 and 747 for the time interval of overlap averages 0.000050 (Figure 7a). The $^{87}Sr/^{86}Sr$ values from site 747 are consistently higher, and the associated curve has almost no structure. Approximately 0.000020 of the offset appears to be attributable to interlaboratory bias that was not corrected by comparing standards; an additional 0.000020-0.000040 may be generated by problems associated with precisely dating slow sedimentation rate sites from high latitudes, where important biostratigraphic marker species are frequently absent, such as site 747.

The youngest portion of the site 926 curve was compared to data from site 758 [*Farrell et al.*, 1995], revealing an excellent similarity in the shape of the curves. There is a consistent offset of ~0.000015 between the two curves, suggesting that there may be an uncorrected interlaboratory bias between these data sets as well. There is no evidence in the site 926 data for the rapid rise in $^{87}Sr/^{86}Sr$ observed at site 758 from 5.9 to 5.8 Ma, although the temporal resolution of the site 926 curve may not be sufficient to resolve this level of structure.

The proposed Sr chemostratigraphic reference section from site 926 is composed of a seventh-order polynomial fit to the $^{87}Sr/^{86}Sr$ data. The $^{87}Sr/^{86}Sr$ values increase at a gentle rate of 20×10^{-6} m.y.$^{-1}$ from ~14 to 11 Ma, increase more rapidly at a rate of 34×10^{-6} m.y.$^{-1}$ from 11 to 8.5 Ma, change very little at a rate of 13×10^{-6} m.y.$^{-1}$ from 8.5 to 6.5 Ma, and then increase at their most rapid rate of 55×10^{-6} m.y.$^{-1}$ from 6.5 to 5 Ma. Errors associated with estimating an age from this curve for a sample of unknown age range from +/- 0.8 m.y. for intervals of rapid change in $^{87}Sr/^{86}Sr$ to +/- 1.6 m.y. a for intervals of minimal change. For the sake of simplicity the curve has also been broken up into four linear segments, and the linear regression equation for each segment is provided. The maximum difference in age estimated from the polynomial fit versus the linear fits is 0.3 m.y.

Acknowledgments. We thank lab assistants D. Kuncicky, N. Harvey, and E. Ahrens for help with the preparation of samples for Sr isotopic analyses and A. Heatherington for assistance with the isotopic measurements. P. Howell, L. Screaton, and A. Heatherington helped set up the programs necessary for the development of nonparametric fits to the data. Thoughtful reviews by T. Moore and K. Miller improved the manuscript. Funding for this project was provided by NSF grants OCE96-29370 (E.E.M.) and EAR97-25311 (J.C.Z. and B.P.F.) and NERC grant GST/2/971 (N.J.S.). Samples were provided by the Ocean Drilling Progam with sponsorship from NSF.

References

Berggren, W.A., D.V. Kent, J.J. Flynn, and V. Couvering, The Neogene, 2, Neogene geochronology and chronostratigraphy, in *The Chronology of the Geologic Record* edited by N.J. Snelling, pp. 211-260, Blackwell, Cambridge, Mass., 1985.

Barton, C.E., and J. Bloemendal, Paleomagnetism of sediments collected during Leg 90, southwest Pacific, *Initial Rep Deep Sea Drill Proj, 90*, 1273-1316, 1986.

Burke, W.H., R.E. Denison, E.A. Hetherington, R.B. Koepnick, H.F. Nelson, and J.B. Otto, Variation of seawater $^{87}Sr/^{86}Sr$ throughout the Phanerozoic, *Geology, 10*, 516-519, 1982

Cande, S.C., and D.V. Kent, A new geomagnetic polarity time scale for the Late Cretaceous and Cenozoic, *J. Geophys. Res., 97*, 13,917-13,951, 1992.

Curry, W.B., N.J. Shackleton, et al., Site 926, *Proc. Ocean Drill. Program Initial Rep., 154*, 153-232, 1995.

DePaolo, D.J., and B.L. Ingram, High-resolution stratigraphy with strontium isotopes, *Science, 227*, 938-941, 1985.

Elderfield, H., Strontium isotope stratigraphy, *Palaeogeogr. Palaeoclimatol. Palaeoecol., 57*, 71-90, 1986.

Farrell, J.W., S.C. Clemens, and L.P. Gromet, Improved chronostratigraphic reference curve of late Neogene seawater $^{87}Sr/^{86}Sr$, *Geology, 23*, 403-406, 1995.

Flower, B.P., J.C. Zachos, and E. Martin, Latest Oligocene through early Miocene isotopic stratigraphy and deep-water paleoceanography of the western equatorial Atlantic: Sites 926 and 929, *Proc. Ocean Drill. Program Sci. Results, 154*, 451-462, 1997.

Hampt, G. and M L. Delaney, Influences on calcite Sr/Ca records from Ceara Rise and other regions: Distinguishing ocean history and calcite recrystallization, *Proc. Ocean Drill. Program Sci. Results, 154*, 491-500, 1997.

Henderson, G.M., D.J. Martel, R.K. O'Nions, and N.J. Shackleton, Evolution of seawater $^{87}Sr/^{86}Sr$ over the last 400 ka: The absence of glacial/interglacial cycles, *Earth Planet. Sci. Lett., 128*, 643-651, 1994

Hess, J., M. Bender, and J.-G.Schilling, Seawater $^{87}Sr/^{86}Sr$ evolution from Cretaceous to present, *Science, 231*, 979-984, 1986.

Hilgen, F.J., W. Krijgsman, C.G. Lourens, A. Sanatarelli, and W.J Zachariasse, Extending the astronomical (polarity) time scale into the Miocene, *Earth Planet. Sci. Lett., 136*, 495-510, 1995.

Hodell, D.A., Progress and paradox in strontium isotope stratigraphy, *Paleoceanography, 9*, 395-398, 1994.

Hodell, D.A., and F. Woodruff, Variations in the strontium isotopic ratio of seawater during the Miocene: Stratigraphic and geochemical implications, *Paleoceanography, 9*, 405-426, 1994.

Hodell, D.A., P.A. Mueller, J.A. McKenzie, and G.A. Mead, Strontium isotope stratigraphy and geochemistry of the late Neogene, *Earth Planet. Sci. Lett., 92*, 165-178, 1989.

Hodell, D.A., P.A. Mueller, and J. Garrido, Variations in the strontium isotopic composition of seawater during the Neogene, *Geology, 19*, 24-27, 1991.

Howarth, R.J., and J.M. McArthur, Statistics for strontium isotope stratigraphy: A robust LOWESS fit to the marine Sr-isotope curve for 0 to 206 Ma, with look-up table for derivation of numeric ages, *J. Geol, 105*, 441-456, 1997.

Imbrie, J., et al., The orbital theory of Pleistocene climate: Support from a revised chronology of the marine $\delta^{18}O$ record, in *Milankovitch and Climate (Part 1), edited by A. Berger et al., NATO ASI Ser. C, Math Phys. Sci., 126*, 269-305, 1984.

Ludwig, K.R., R.B. Halley, K.R. Simons, and Z.E. Peterman, Strontium-isotope stratigraphy of Enewetak Atoll, *Geology, 16*, 173-177, 1988.

McKenzie, J.A., D.A. Hodell, P.A. Mueller, and D.W. Mueller, Application of strontium isotopes to late Miocene-early Pliocene stratigraphy, *Geology, 16*, 1022-1025, 1988.

Mead, G.A., and D.A. Hodell, Controls on the $^{87}Sr/^{86}Sr$ composition of seawater from the middle Eocene to Oligocene: Hole 689B, Maud Rise, Antarctica, *Paleoceanography, 10*, 327-346, 1995.

Miller, K.G., and D.V. Kent, Testing Cenozoic eustatic changes: The critical role of stratigraphic resolution, *Spec. Publ. Cushman Found. Foraminiferal Res., 24*, 51-56, 1987.

Miller, K.G., M.D. Feigenson, J.D. Wright, and B.M. Clement, Miocene isotope reference section, Deep Sea Drilling Project Site 608: An evaluation of isotope and biostratigraphic resolution, *Paleoceanography, 6,* 33-52, 1991.

Oslick, J.S., K.G.Miller, M.D. Feigenson, and J.D. Wright, Oligocene-Miocene strontium isotopes: Stratigraphic revisions and correlations to an inferred glacioeustatic record, *Paleoceanography, 9,* 427-444, 1994.

Palmer, M.R., and H. Elderfield, Sr isotope composition of sea water over the past 75 myr., *Nature, 314,* 526-528, 1985.

Pearson, P.N., and W.P. Chaisson, Late Paleocene to middle Miocene planktonic foraminifer biostratigraphy of the Ceara Rise, *Proc. Ocean Drill. Program Sci. Results, 154,* 33-68, 1997

Pin, C., and C. Bassin, Evaluation of a Sr-specific extraction chromatographic method for isotopic analysis in geologic materials, *Anal. Chim Acta, 269,* 249-255, 1992.

Shackleton, N.J., and S. Crowhurst, Sediment fluxes based on an orbitally tuned time scale 5 Ma to 14 Ma, Site 926, *Proc. Ocean Drill. Program Sci. Results, 154,* 69-82, 1997.

Shackleton, N.J , and M.A. Hall, The late Miocene stable isotope record, Site 926, *Proc. Ocean Drill. Program Sci. Results, 154,* 368-374, 1997

Shackleton, N.J , and J. Imbrie, The $\delta^{18}O$ spectrum of oceanic deep water over a five decade band, *Clim. Change, 16,* 217-230, 1990.

Shackleton, N.J., S. Crowhurst, T. Hagelberg, N G Pisias, and D.A Schneider, A new late Neogene time scale: Application to Leg 138 sites, *Proc Ocean Drill. Program, Sci. Results, 138,* pp 73-101, 1995

Shackleton, N.J , S. Crowhurst, T. Hagelberg, N G. Pisias, and D.A. Schneider, A new late Neogene time scale· Application to Leg 138 sites, *Proc Ocean Drill. Program Sci. Results, 138,* 73-101, 1995.

Wright, J.D., and K.G. Miller, Miocene stable isotope stratigraphy, Site 747, Kerguelen Plateau, *Proc. Ocean Drill. Program Sci. Results, 120,* 855-866, 1992.

B.P. Flower, Department of Marine Science, University of South Florida, 140 Seventh Avenue South, St. Petersburg, FL 33701. (email: bflower@seas.marine.usf.edu)

E.E. Martin, Department of Geology, University of Florida, 241 Williamson Hall, Gainesville, FL 32611-2120. (e-mail: emartin@geology.ufl.edu)

N.J. Shackleton, University of Cambridge, Godwin Laboratory, New Museums Site, Pembroke St., Cambridge CB3SA, UK. (email: njs5@cam.ac.uk)

J.C. Zachos, Earth Sciences Department, University of California, Santa Cruz, CA 95064. (email: jzachos@emerald.ucsc.edu)

(Received June 22, 1998;
revised October 12, 1998,
accepted October 19, 1998.)